ISO SPECTROSCOPY OF YOUNG STELLAR OBJECTS

E.F. van Dishoeck[1], J.H. Black[2], A.C.A. Boogert[3], A.M.S. Boonman[1], P. Ehrenfreund[1], P.A. Gerakines[4], Th. de Graauw[5], F.P. Helmich[1,6], J.V. Keane[3], F. Lahuis[5], W.A. Schutte[1], A.G.G.M. Tielens[3,5], D.C.B. Whittet[4], C.M. Wright[1], M.E. van den Ancker[7], G.A. Blake[8], M. Creech-Eakman[8], L.B.F.M. Waters[7], & P.R. Wesselius[5]

[1] Leiden Observatory, P.O. Box 9513, 2300 RA Leiden, The Netherlands
[2] Onsala Space Observatory, S–43992 Onsala, Sweden
[3] Kapteyn Astronomical Institute, P.O. Box 800, 9700 AV Groningen, The Netherlands
[4] Dept. of Physics, Applied Physics and Astronomy, Rensselaer Polytechnic Institute, Troy NY 12180, USA
[5] SRON, P.O. Box 800, 9700 AV Groningen, The Netherlands
[6] Earth Observations Division, SRON, Sorbonnelaan 2, 3584 CA Utrecht, The Netherlands
[7] Astronomical Institute, University of Amsterdam, Kruislaan 403, 1098 SJ Amsterdam, The Netherlands
[8] Div. of Geological & Planetary Sciences, California Institute of Technology, Pasadena, CA 91125, USA

ABSTRACT

Observations of gas-phase and solid-state species toward young stellar objects (YSOs) with the spectrometers on board the Infrared Space Observatory are reviewed. The excitation and abundances of the atoms and molecules are sensitive to the changing physical conditions during star-formation. In the cold outer envelopes around YSOs, interstellar ices contain a significant fraction of the heavy element abundances, in particular oxygen. Different ice phases can be distinguished, and evidence is found for heating and segregation of the ices in more evolved objects. The inner warm envelopes around YSOs are probed through absorption and emission of gas-phase molecules, including CO, CO_2, CH_4 and H_2O. An overview of the wealth of observations on gas-phase H_2O in star-forming regions is presented. Gas/solid ratios are determined, which provide information on the importance of gas-grain chemistry and high temperature gas-phase reactions. The line ratios of molecules such as H_2, CO and H_2O are powerful probes to constrain the physical parameters of the gas. Together with atomic and ionic lines such as [O I] 63 μm, [S I] 25 μm and [Si II] 35 μm, they can also be used to distinguish between photon- and shock-heated gas. Finally, spectroscopic data on circumstellar disks around young stars are mentioned. The results are discussed in the context of the physical and chemical evolution of YSOs.

Key words: molecules; ices; silicates; embedded YSOs; shocks; PDRs; circumstellar disks.

1. INTRODUCTION

The formation of stars occurs deep inside molecular clouds, and is often obscured by hundreds of magnitudes of extinction. In recent years, ground-based infrared and (sub-)millimeter observations have provided a broad outline of the different stages of star formation (see Fig. 1). The process starts with the collapse of a molecular cloud core, and is followed by an embedded phase in which both accretion onto the protostar and supersonic outflow occur simultaneously. This eventually leads to the clearing stage in which the envelope is dispersed and the young star is revealed optically, in most cases surrounded by a remnant circumstellar accretion disk (e.g., Shu et al. 1993). Intense ultraviolet radiation from the star-disk boundary layer and the young star itself can heat the surrounding gas and affect the abundances through photodissociation and photoionization (e.g., Hollenbach & Tielens 1997). The tremendous range in physical conditions in these different phases, with densities from 10^4 to 10^{13} cm^{-3} and temperatures from 10–10,000 K, affect the abundances and excitation of atoms and molecules. Spectroscopic data therefore contain an enormous amount of information with which to unravel the physical and chemical evolution during star formation.

Observations with the spectrometers on board the Infrared Space Observatory (ISO) in the 2.4–200 μm region are particularly well suited to address several aspects of the physical and chemical properties of YSOs. First, the infrared wavelength region is rich in diagnostic lines of atoms, ions and molecules, which can be used to constrain the physical parameters and assess the importance of different processes such as shocks versus ultraviolet radiation. Second, the broad wavelength coverage, unhindered by the Earth's atmosphere, provides an unbiased overview of the major gas- *and* solid-state species in star-forming regions, and allows an inventory of the major elements (C, O, N, ...) to be made. Third, the evolution of the molecular composition from dark cloud cores to the formation of circumstellar disks and new planetary systems can be probed, thus providing insight into the origin of chemical compounds in our own so-

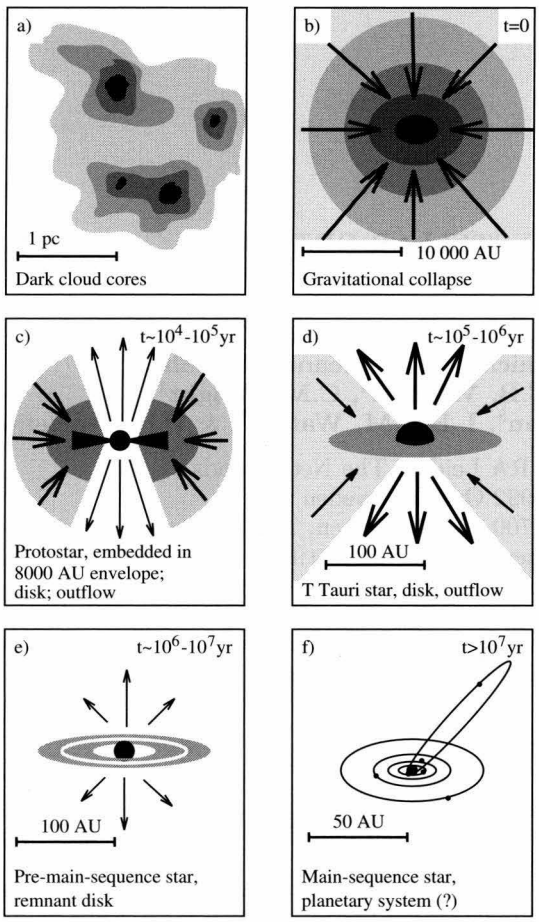

Figure 1. Schematic overview of the various stages in the formation of a low-mass star (Hogerheijde 1998, based on Shu et al. 1993).

lar system (see van Dishoeck & Blake 1998, Langer et al. 1999, van Dishoeck & Hogerheijde 1999 for overviews).

The main limitations of the ISO spectrometers compared with ground-based instruments are their relatively low spatial and spectral resolution. The sizes of the different physical components in YSOs range from less than a few arcsec (circumstellar disks, hot cores) to $\sim 30''$ or larger (outer envelopes, outflows), all of which are blurred together in the ISO spectrometer beams. In addition, the spectral resolution is generally too poor to obtain kinematic information, except for lines in outflows observed with the Fabry-Pérots. Careful modelling is therefore required to extract the relevant information.

In this review, the ISO spectroscopic observations of the envelopes around YSOs at various evolutionary stages are briefly discussed. Observations with the Short Wavelength Spectrometer (SWS) are emphasized, but references to relevant data obtained with the Long Wavelength Spectrometer (LWS) presented elsewhere in these proceedings are made throughout the paper. Additional information can be found in the proceedings of the conferences on "Star Formation with the ISO Satellite" (Yun & Liseau 1998), "ISO's View on Stellar Evolution" (Waters et al. 1998), and "Analytical Spectroscopy with ISO" (Heras et al. 1997).

2. MID-INFRARED SPECTROSCOPY: ORION IRC2 AS AN EXAMPLE

A multitude of atomic, ionic and molecular lines occur at mid-infrared wavelengths which can be used to probe the environment of YSOs. At shorter wavelengths ($< 10\,\mu$m), atomic recombination lines such as those of H I into levels n=5, 6 and 7 appear. In addition, atomic fine-structure lines of a large variety of atoms and ions are found throughout the mid- and far-infrared, including those of [S I] – [S IV], [Ne II], [Ne III], [Ne V], [Si II], [O I], [O III], and [C II]. The line ratios can be used to constrain the temperature and density of the ionized gas, as well as the spectrum and characteristics of the ionizing source(s) (e.g., Genzel et al. 1998).

The physical structure of warm, molecular gas can be studied with the ISO-SWS through the pure rotational lines of the dominant interstellar molecule H_2 at 28.22 S(0), 17.03 S(1), 12.3 S(2), 9.66 μm S(3), etc. In addition, lines in the H_2 v=1–0, 2–1, ... vibrational bands are found in the 2–4 μm range (e.g., Black & van Dishoeck 1987). The lowest rotational lines of heavy molecules like CO lie at submillimeter wavelengths, but the higher transitions starting at CO J=14→13 are covered by the LWS. H_2O also has pure rotational lines in the LWS and SWS wavelength range. Together, the H_2, CO and H_2O lines are powerful probes of shocks and PDRs.

Vibrational bands of most gas-phase molecules such as CO, CO_2, CH_4 and H_2O occur in the near- to mid-infrared wavelength range, primarily at $\lambda < 20\,\mu$m. In general, a molecule with N atoms has $3N - 5$ (if linear) or $3N - 6$ (if non-linear) vibrational modes, and the broad spectral coverage of ISO allows more than one band to be detected.

The mid-infrared wavelength range is particularly powerful at probing the composition of interstellar dust, which lacks strong features in the submillimeter part of the spectrum. Vibrational bands of solid-state species can be distinguished from those of gas-phase molecules because they do not have the rotational substructure of the bands, because of their large widths, and because their positions are slightly shifted (see Fig. 7). Bands of silicates, ices and large molecules such as polycyclic aromatic hydrocarbons (PAHs) are seen prominently in the infrared (see papers by Tielens, Waters, Waelkens, and d'Hendecourt et al. in these proceedings).

The wealth of information contained in mid-infrared spectra of YSOs is illustrated in Fig. 2, which shows the full mid-infrared spectrum from 2.4-45.2 μm obtained toward Orion IRc2 with the ISO–SWS (van Dishoeck et al. 1998a). Orion-IRc2 is the nearest, best studied region of massive star formation in the Galaxy, and therefore also serves as an important template for more distant star-forming regions in external galaxies. Most of the spectral features discussed above are seen in the Orion spectrum. The various lines probe the different components contained in the ISO–SWS beam, which also covers the BN object and which varies from $14'' \times 20''$ at the shorter wavelengths, to $20'' \times 33''$ at the longer wavelengths (see Fig. 3). The H II region lying in front of the molecular cloud is probed through the atomic and ionic lines, whereas the PDR at the interface of

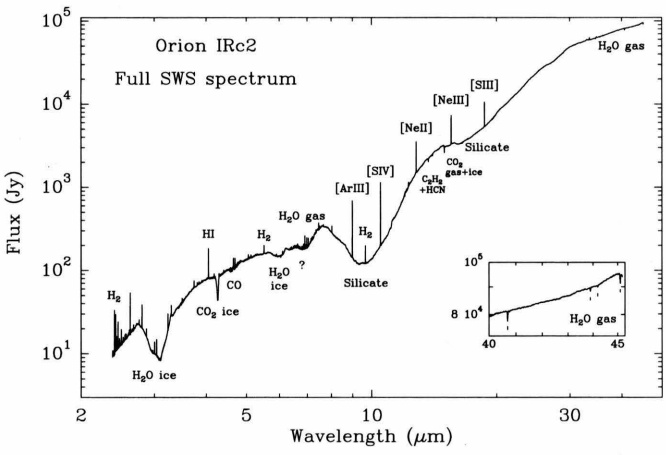

Figure 2. Complete ISO–SWS grating spectrum centered on Orion IRc2 at a resolving power R=1300–2500. The principal absorption and emission features are indicated. The inset shows a blow-up of the 40–45 μm region, in which several gas-phase H_2O absorption lines can be seen (van Dishoeck et al. 1998a).

the ionized and molecular gas is seen by PAH emission. The powerful shock or "plateau" originating near IRc2 results in strong H_2 and H_2O lines, and the quiescent molecular ridge is observed by absorption of silicates and H_2O- and CO_2-ices. The rich spectroscopy of the Orion shock is also beautifully revealed by ISO-SWS spectra taken at the peak I and II positions, about 30″ offset from IRc2 (Rosenthal et al., these proceedings, Wright et al. 1999a).

Not all YSOs have spectra as rich as that of Orion IRc2. Often only one or two of the physical components dominate. In the following, examples of objects at various evolutionary stages will be discussed. H II regions, which reveal strong ionic lines and PAH features, are reviewed by Cox et al. (these proceedings) and, e.g., Roelfsema et al. 1996.

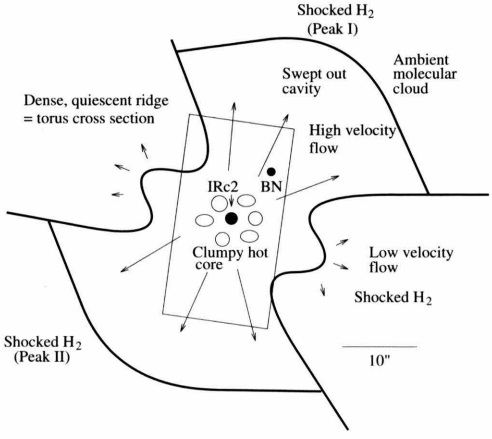

Figure 3. Schematic illustration of the Orion IRc2/BN region. The figure represents a cross section in the plane of the sky. The SWS aperture during the ISO observations is indicated.

3. COLD OUTER ENVELOPES AROUND YSOs

The gas and dust in circumstellar envelopes are best probed through infrared absorption lines toward the embedded YSOs themselves. The young stars heat the dust in their immediate surroundings to a few hundred K, providing a continuum against which the cooler foreground species can be seen in absorption. Such observations provide a powerful complement to submillimeter emission line studies of these regions (Evans et al. 1991, Carr et al. 1995, van der Tak et al. 1999). Only a pencil beam toward the source is probed in absorption, and both the gas and the dust can be observed along the same line-of-sight.

3.1. Overview of ice features

During the quiescent cloud and collapse phases, the densities are high and the temperatures low, so that the timescales for gas-phase atoms and molecules to collide with the grains and stick are short, less than 10^5 yr. Subsequent hydrogenation and oxidation reactions on the grain surfaces form new species. Specifically, O, C and N are expected to react with H to form H_2O, CH_4 and NH_3, whereas CO can be driven into H_2CO, CH_3OH or CO_2 (e.g., Tielens & Hagen 1982). The grain cores in star-forming regions are therefore expected to be surrounded by mantles containing a variety of ices. H_2O-ice was discovered in the 1970's by ground-based observations and the study of ices was subsequently pursued from ground and airborne platforms (e.g., Willner et al. 1982, Tielens et al. 1991). The main advantage of ISO is that it provides the first complete, unbiased census. This is nicely demonstrated by the full ISO-SWS spectra of deeply embedded massive YSOs such as NGC 7538 IRS9 (Whittet et al. 1996), GL 7009S (d'Hendecourt et al. 1996), NGC 7538 IRS1 (Strazzula et al. 1998), and W 33A (Gibb et al. 1999), which indeed show strong absorptions by a wide variety of ices (see Fig. 4).

Overviews of recent ISO–SWS observations of ices have been given by Tielens & Whittet (1997), Ehrenfreund et al. (1997), van Dishoeck et al. (1998b), Ehrenfreund (1999), Schutte (1999), and d'Hendecourt et al. (these proceedings). Ices have also been observed with ISOPHOT-S (e.g., Guertler et al. 1996) and with the ISOCAM-CVF (André et al., in preparation). The higher sensitivity of these instruments allows observations of weaker sources, but their low spectral resolution prevents a detailed analysis of the line profiles. Nevertheless, a rough comparison of spectral features and abundances between low- and high-mass objects will be very interesting when such data become available.

In Fig. 4, the 2.5–20 μm ISO-SWS spectrum toward the deeply embedded massive YSO W 33A is shown at an average resolving power of 1000 (Gibb et al. 1999). Molecules such as solid H_2O, CO, CH_3OH, OCS and 'XCN'/OCN^- were known from ground-based observations, but ISO has detected several new species. The complete spectral coverage makes the identifications more secure, since more than one vibrational band can be detected. One of the strongest absorptions observed toward all YSOs

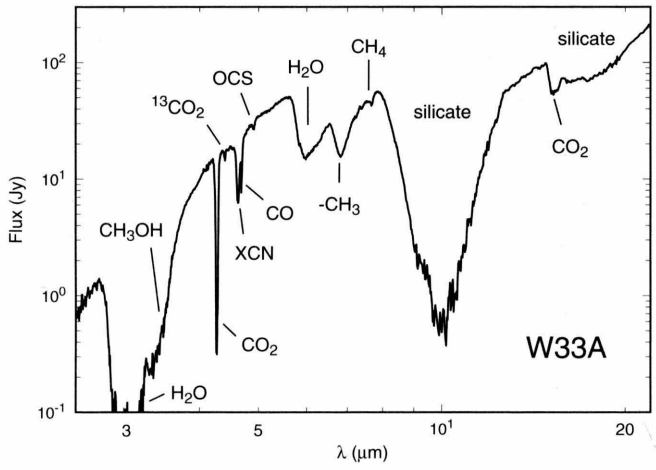

Figure 4. ISO-SWS spectrum of the deeply embedded massive YSO W 33A. A variety of ice mantle and refractory grain core features are evident (Gibb et al. 1999).

is the ν_3 stretching mode at 4.27 μm due to solid CO_2, for which the corresponding ν_2 bending mode lies at 15.2 μm (e.g., de Graauw et al. 1996, d'Hendecourt et al. 1996, Strazzula et al. 1998, Gerakines et al. 1999). The abundance of CO_2 ice with respect to H_2O ice is remarkably constant at about 18%. The $^{13}CO_2$ band is readily detected as well (Boogert et al. 1999). Other new ISO identifications include solid CH_4 (Boogert et al. 1998), HCOOH and perhaps $HCOO^-$ (Schutte et al. 1996, 1999). H_2CO, however, has an abundance of at most a few % (Ehrenfreund et al. 1997). As the data reduction continues to improve, weaker features may be discovered which provide constraints on minor components of the ices. The principal carrier of the strong 6.8 μm feature is still unidentified, although it is likely that CH_3OH and perhaps NH_4^+ and/or carbonates contribute (Demyk et al. 1998, Dartois et al. 1999, Keane et al., these proceedings). Laboratory simulations continue to be essential for the interpretation of such data (d'Hendecourt et al., these proceedings); an overview of the Leiden Observatory Laboratory data base can be found at `<http://www.strw.leidenuniv.nl/~lab/>`.

3.2. The Oxygen budget

The ISO spectra allow a more accurate determination of the abundances of species and the budgets of the various elements, especially that of oxygen. In general, the total amount of oxygen available for gas and ices (i.e., not locked up in silicates) is 3.3×10^{-4} with respect to hydrogen, based on ultraviolet absorption line observations of O I in diffuse clouds (Meyer et al. 1998). Schutte (1999) shows that in the Taurus dark cloud toward the background star Elias 16, ~85% of the oxygen can be accounted for. About 40% is in H_2O ice, about 25% in CO-, CO_2- and other oxygen-containing ices, and about 20% in gas-phase CO. This analysis assumes that the observed silicate optical depth is a good measure of the total hydrogen column density along the line of sight.

Solid O_2 is not a major component in YSOs, as demonstrated by Vandenbussche et al. (1999) for the low-mass YSO R CrA IRS2 and the high-mass YSO NGC 7538 IRS9. For these objects, the ices and gas-phase CO account for ~60–70% of the available oxygen, leaving up to 40% undetected. Since the limits on gas-phase O_2 are low, both from balloon experiments (O_2/CO<0.04, Olofsson et al. 1998) and from the first SWAS results (O_2/CO<0.03–0.06, Melnick et al. 1999), the missing oxygen is most likely in the form of atomic gas-phase O I, as shown toward SgrB2 with the ISO-LWS (Baluteau et al. 1997). In warm ($T > 300$ K) dense gas, a large fraction of the oxygen may be driven into gas-phase H_2O (Harwit et al. 1998, see Section 5).

3.3. Ice heating and segregation

The large and systematic data base on ices obtained with the ISO-SWS is particularly useful for studies of the evolution of ices. It is well known from ground-based solid CO data that ice mantles are not homogeneous but consist of different phases, or layers, including a water-rich polar phase and a CO-rich apolar phase (e.g., Tielens et al. 1991, Schutte 1999). The CO_2 bending mode at 15 μm is an especially sensitive diagnostic of the ice environment and the degree of thermal processing (Gerakines et al. 1999, Ehrenfreund et al. 1998a,b). Pure CO_2-ice at 10 K has a characteristic double-peak structure at 15.15 and 15.25 μm, whereas CO_2 mixed with H_2O and other species has a broad, mostly featureless profile with a shoulder at 15.4 μm. This latter band is due to complexes of CO_2 with another polar molecule, most likely CH_3OH. Laboratory experiments show that upon heating of H_2O:CH_3OH:CO_2 mixtures, the broad asymmetric profile converts to a multipeak structure and the 15.4 μm band disappears due to segregation of the ices (Ehrenfreund et al. 1998b). This is very similar to the structure observed in ISO spectra, of which a subsample is shown in Fig. 5. The systematic evolution of the profile with increasing temperature is a strong indication that thermal processing and ice segregation are important in the inner envelopes of embedded YSOs. A similar conclusion is reached from a detailed study of the $^{13}CO_2$ 4.38 μm stretching band, which is much weaker and therefore easier to analyze than the heavily saturated $^{12}CO_2$ 4.27 μm feature (Boogert et al. 1999). In addition to temperature, time also plays an important role in the interstellar case: the more evolved the object, the larger the fraction of ices affected by the heating. A schematic view of the different ice phases in envelopes around YSOs is shown in Fig. 6.

4. WARM INNER ENVELOPES AROUND YSOs

Young stars heat their surrounding envelopes, resulting in a temperature gradient throughout the surrounding gas and dust. Self-consistent calculations of the radial temperature structure include those of Doty & Neufeld (1997), Kaufman et al. (1998) and van der Tak et al. (1999). According to these models, the temperature follows a $\propto r^{-0.4}$ law in the outer envelope, but steepens in the inner part where

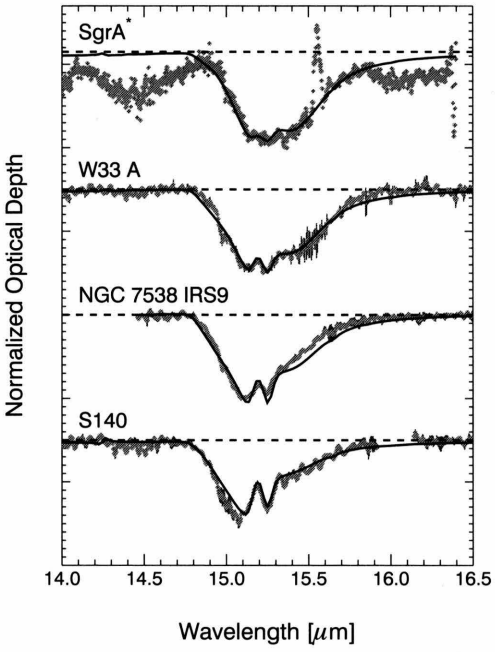

Figure 5. ISO–SWS spectra of the CO_2 bending mode near 15 μm, illustrating the thermal evolution of interstellar ices. The sources are displayed in order of increasing gas temperature as derived from CO observations (Mitchell et al. 1990). Solid lines are fits based on laboratory data for an ice mixture H_2O:CH_3OH:CO_2=1:1:1 at various temperatures (Gerakines et al. 1999).

the dust becomes optically thick at infrared wavelengths. The gas temperature is expected to closely follow the dust temperature through gas-grain collisions, although cooling through atomic ([O I] 63 μm, [C II] 158 μm) and molecular (CO, H_2O) lines can occur as well. For a $\sim 10^5$ $L_\odot$ source, the region where $T_d \approx T_{\rm gas} > 90$ K extends to $\sim 10^{16}$ cm, whereas the region with $T_d > 20$ K extends to $\sim 5 \times 10^{17}$ cm. All ices are evaporated in the inner part of the envelopes, i.e., within a few arcsec for a typical distance of 1 kpc. In this so-called "hot core" region, a rapid high temperature gas-phase chemistry occurs in which a large fraction of the available oxygen is driven into H_2O at temperatures above ~230 K (Charnley 1997). In

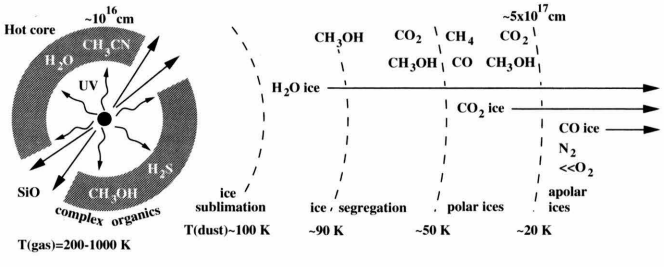

Figure 6. Schematic illustration of the temperature structure of the envelopes of YSOs and the different ice phases due to heating and thermal desorption (van Dishoeck & Hogerheijde 1999).

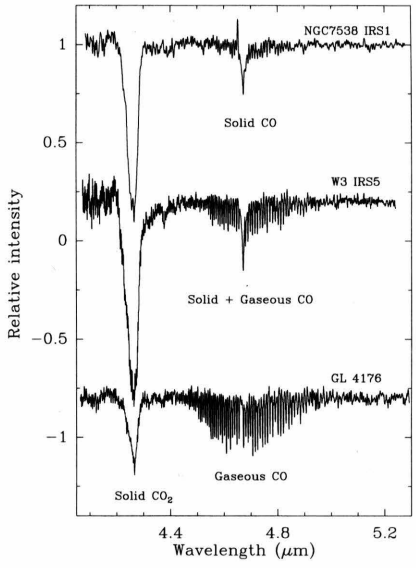

Figure 7. ISO-SWS spectra of solid-state CO_2 and solid- and gas-phase CO absorption toward embedded massive YSOs, illustrating the evaporation of ices and the development of a "hot core" region near W 3 IRS5 and AFGL 4176 (van Dishoeck et al. 1998b).

addition to radiative heating by the young star, the interaction of the outflow with the envelope can result in enhanced temperatures. At the positions of direct impact, the temperature is raised to several thousand K or more, depending on the speed of the shock. In addition, the walls along the outflow cavity are heated due to slower, oblique shocks. Turbulent mixing results in slow entrainment of the gas and dust with removal of the ice mantles.

The warm envelopes have been probed through absorption lines with the SWS, and by emission and absorption lines with the LWS.

4.1. SWS absorption observations

Ground-based observations of the vibrational band of gas-phase CO at 4.7 μm by Mitchell et al. (1990) have revealed the presence of cold ($T_{\rm ex} = 20 - 60$ K) and warm ($T_{\rm ex}$=200–1000 K) gas along the lines of sight toward massive YSOs. Although the ISO–SWS has much lower spectral resolution, warm gas-phase CO is detected toward several YSOs and can be readily distinguished from solid CO (Figure 7). Note that the CO excitation temperatures derived from the absorption data may differ from the kinetic temperatures because of the power-law structure of the envelope and because the higher levels are difficult to keep collisionally excited (van der Tak et al. 1999). Radiative pumping may be important as well, driving $T_{\rm ex}$ to the temperature of the radiation field which reflects hotter dust closer in. Nevertheless, their values allow a relative ordering of the sources by temperature.

The ISO-SWS has allowed searches for other gas-phase molecules, in particular H_2O and CO_2 which cannot be observed from the ground and which are among the dominant O- and C-containing species.

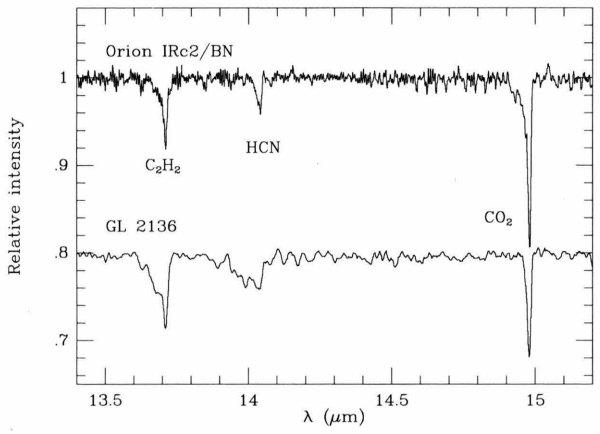

Figure 8. Absorption by gas-phase CO_2, C_2H_2 and HCN toward Orion IRc2/BN and GL 2136. Note the much broader C_2H_2 and HCN profiles toward GL 2136, indicating much higher excitation temperatures (Boonman et al. 1999, Lahuis & van Dishoeck 1997).

One of the early SWS surprises included the detection of abundant (~few $\times 10^{-5}$ with respect to H_2), hot ($T_{ex} \approx 300$ K) gas-phase H_2O absorption toward a number of YSOs (Helmich et al. 1996, van Dishoeck & Helmich 1996, van Dishoeck 1998). In contrast, the abundance of gas-phase CO_2 was found to be much lower, a few $\times 10^{-7}$ (van Dishoeck et al. 1996, van Dishoeck 1998). Gas-phase CH_4 (Boogert et al. 1998), C_2H_2 and HCN (Lahuis & van Dishoeck 1997, 1999) have also been detected, with abundances up to 10^{-6} and excitation temperatures ranging from ~ 100 K (CH_4) up to 1000 K (HCN, C_2H_2) in some YSOs (see Fig. 8). The gas-phase results, combined with the solid-state data for the same lines of sight, allow the gas/solid ratios to be determined (van Dishoeck et al. 1996, Dartois et al. 1998, van Dishoeck 1998). Significant variations are found between the different objects, which are not correlated with the YSO luminosities (van der Tak et al. 1999, Boogert et al. 1999). Instead, evolutionary effects appear to play a role, indicating the gradual heating and evaporation of ices in the inner parts of the warm envelopes (see also Section 5, Figure 12).

4.2. LWS emission observations

Emission line observations of a variety of YSOs with a range of luminosities at different evolutionary stages have been performed within the LWS central program. An overview of the results is given by Saraceno et al. (these proceedings, and references cited). The youngest, deeply embedded low-luminosity sources have very rich spectra with many molecular lines due to CO, H_2O and OH detected. In most objects, the total luminosity in the CO lines, and thus the total cooling, is higher than that in the H_2O or OH lines. In contrast, high luminosity sources show strong atomic and ionic lines, in particular [C II] 158 μm and [O I] 63 and 145 μm emission, with weaker molecular lines. The only exception is formed by massive sources in the Galactic center region, which show strong H_2O and OH absorption lines (e.g., Baluteau et al. 1997). An example of part of the LWS grating spectrum toward the high-mass YSOs W 3 IRS5 and GL 2591 are presented in Fig. 9. Part of the apparent lack of molecular lines in high-mass objects may be caused by their strong continuum emission, resulting in low line/continuum ratios at low spectral resolution.

Ceccarelli et al. (1998) and Nisini et al. (1999a,b) (see Saraceno et al. 1999 for a summary) show that the observed CO rotational excitation for most objects can be fitted with temperatures of a few hundred K and densities of $\sim 10^6$ cm^{-3} within a region some 1″–10″ in size, although alternative fits with higher temperatures of 500–1000 K and lower densities extended over a larger area are possible as well. The former conditions correspond well with those found for the inner envelopes of high mass YSOs from the absorption line data, whereas the latter parameters are more typical of extended outflows. Further modelling of the combined absorption and emission line data is needed to distinguish between these two interpretations, taking into account the temperature gradient through the envelope.

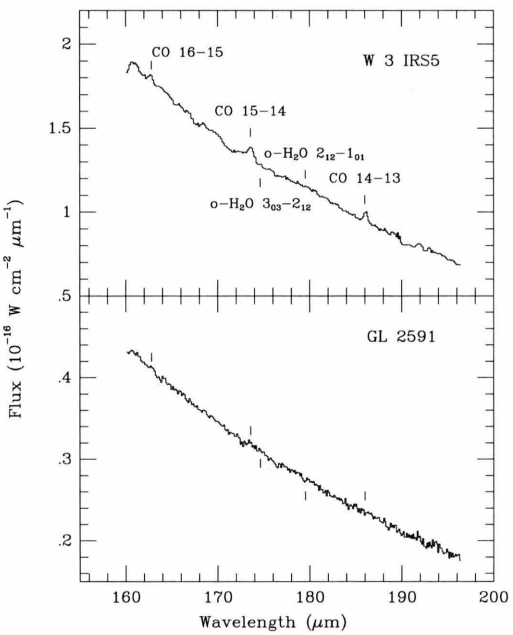

Figure 9. Top: Part of the LWS01 grating spectrum toward the massive YSO W 3 IRS5, showing CO emission lines but no H_2O lines; Bottom: Part of the LWS01 spectrum toward GL 2591, showing no CO emission lines but perhaps weak H_2O $2_{12} - 1_{01}$ absorption at 179 μm (Wright et al. 1997b).

5. H_2O AS A PROBE OF WARM GAS

The H_2O molecule is a particularly powerful diagnostic of the physical and chemical structure of star-forming regions. H_2O is predicted to be the dominant oxygen-bearing species in warm, dense gas, such as found in shocks and hot cores, because most of the

available oxygen is driven into H_2O at high temperatures (T >230 K) through the reactions $O + H_2 \rightarrow OH + H$ and $OH + H_2 \rightarrow H_2O + H$ (Charnley 1997). In addition, the H_2O level populations are sensitive to collisions and to pumping by far-infrared radiation due to warm dust. Finally, H_2O can contribute to the cooling and heating of the gas (e.g., Neufeld & Kaufman 1993). Previous ground- and airborne observations suggest that the H_2O abundance is low, $< 10^{-7}$, in quiescent clouds (e.g., Zmuidzinas et al. 1995), but is increased to $10^{-5} - 10^{-4}$ in warm gas (e.g., Cernicharo et al. 1994).

Because ground-based observations are hampered by the Earth's atmosphere, ISO has provided the first opportunity to observe a large variety of non-masing H_2O lines in YSOs, including both lower and higher excitation lines. The pure rotational lines are observed with the LWS and SWS, whereas the vibration-rotation lines are seen only with the SWS. Although ISO was not sensitive to cold H_2O, it was well suited to probe H_2O in warm gas. An important limitation is the low spectral resolution, which prevents detection of the weaker, optically thin isotopic lines in most sources except Orion and SgrB2.

ISO–LWS observations at 80–200 μm toward shocks and bipolar outflows associated with low-mass objects such as HH 54 (Liseau et al. 1996), L1448 (Nisini et al. 1998), and IRAS 16293 –2422 (Ceccarelli et al. 1998) show a large variety of H_2O lines. In high mass objects, a wealth of H_2O emission lines originating from levels up to 1000 K above ground has been detected with the LWS toward Orion-KL and SgrB2 (Harwit et al. 1998, Cernicharo et al. 1997a,b), and are discussed in more detail by Cernicharo et al. in these proceedings.

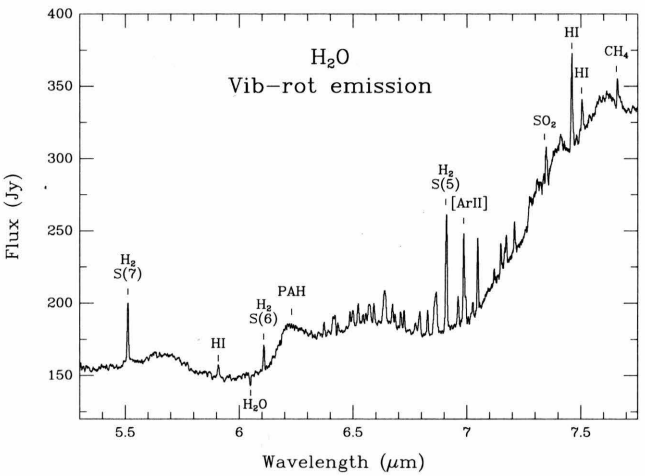

Figure 10. Enlargement of the ISO-SWS spectrum toward IRc2 in the 5.3–7.8 μm range, showing the H_2O ν_2 vibration-rotation lines, as well as several H_2 pure rotational lines (van Dishoeck et al. 1998a, González-Alfonso et al. 1998).

In the ISO-SWS range, H_2O is detected in absorption through its vibrational bending mode at 6 μm in several objects (see Section 4). Surprisingly, however, the LWS grating spectra of the same objects show no or only weak H_2O emission lines (Wright et al. 1997b, see Fig. 9). The most plausible interpretation is that the abundant, warm H_2O in these objects is limited to a small region only a few arcsec in size, such as the hot cores. This is in contrast with Orion and SgrB2, where H_2O emission with the LWS is seen over scales of several arcmin.

Toward Orion IRc2/BN, the H_2O ν_2 band is seen both in emission and absorption (van Dishoeck et al. 1998a), in a pattern which can be explained by a resonant scattering model in a circumstellar shell around BN (González-Alfonso et al. 1998) (see Fig. 10). At longer wavelengths, 25–45 μm, several H_2O pure rotational lines are seen in absorption toward IRc2 (Wright et al. 1999b, see Fig. 2). Fabry-Pérot data of the lines show that the H_2O absorption arises in the outflow centered at IRc2, with some lines showing a characteristic P-Cygni profile (see Fig. 11). At positions away from the strong continuum sources or in the larger LWS beam, the lines appear in emission (Harwit et al. 1998, Cernicharo et al., these proceedings).

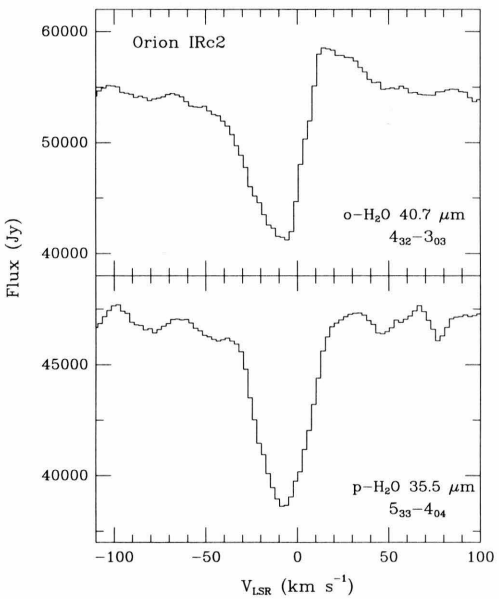

Figure 11. Examples of high-J absorption lines toward Orion IRc2 observed with the ISO-SWS Fabry-Pérot at $\sim$ 10 km s^{-1} resolution. The broad profiles indicate that the H_2O absorption originates in the outflow (Wright et al. 1999b).

The preliminary conclusion from all these data is that the H_2O abundance is high in warm regions, $\sim 10^{-5}$ up to a few $\times 10^{-4}$ with respect to H_2. The temperature and density are high, > 100 K and > 10^5 cm^{-3}, in most regions where the molecule has been detected. The main exception is GL 7009S, where gas-phase H_2O has an excitation temperature of only 20–50 K (Dartois et al. 1998). Whether the H_2O is subthermally excited or whether this reflects the low kinetic temperature in a very young source remains to be determined.

Fig. 12 summarizes the H_2O abundances derived from the 6 μm absorption line data, which involve the fewest model assumptions (van Dishoeck 1998).

The results indicate that two mechanisms play a role in enhancing the gas-phase H_2O abundance over the quiescent values. Evaporation of ices starts at dust temperatures T_d above 90 K and is responsible for the increase in abundance from $< 10^{-7}$ in cold clouds to a few $\times 10^{-6}$. Because the total gas plus solid H_2O abundance is less in these objects than in the coldest objects, at least part of the gas-phase H_2O is likely destroyed upon evaporation, probably to form atomic oxygen. The second jump in abundance results from high-temperature gas-phase chemistry above 230 K through the O + H_2 and OH + H_2 reactions. Note that the absorption data are averaged along the line of sight, so that local abundances could be higher than those shown in Fig. 12.

Analysis of the H_2O emission lines in the LWS requires a good radiative transfer code to handle the optically thick lines, as well as a detailed physical model of the source. Depending on the adopted method, the inferred abundances differ by up to an order of magnitude. Further modelling of the full LWS and SWS data set on objects such as Orion is required to determine whether abundances as high as 3×10^{-4} as inferred by Harwit et al. (1998) are indeed reached.

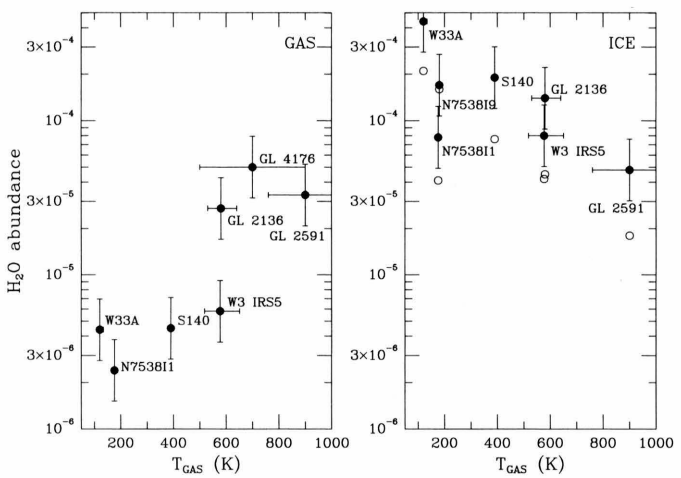

Figure 12. Left: Observed H_2O abundances in the warm gas, $N(H_2O)/N_{\rm warm}(H_2)$, as functions of the warm gas temperature $T_{\rm gas}$ determined from the CO excitation by Mitchell et al. (1990). This temperature is an upper limit to the kinetic temperature (see text). Right: Observed solid H_2O abundances with respect to total H_2 (open symbols) and cold H_2 (filled symbols), as functions of $T_{\rm gas}$ (van Dishoeck 1998).

Another interesting conclusion based on the LWS data is that H_2O is generally not the major coolant of the gas compared with CO and/or H_2. Moreover, the limited LWS and SWS Fabry-Pérot data indicate that the H_2O line formation is complex, with self-absorptions or reversals observed for several cases (Cernicharo et al. 1997, Wright et al. 1997b, 1999b). Lines originating from the lowest energy levels, such as the $2_{12} - 1_{01}$ line at 179 μm, occur in absorption in regions with colder foreground gas. It provides a warning that the strengths of many other unresolved lines, including the [O I] 63 μm line, may be affected by self-absorptions. Although this complicates the modelling, it implies that, eventually, more information about the geometry of the source can be extracted from the data.

6. PDRS AND SHOCKS

Shocks due to outflows penetrating through the envelopes and PDRs caused by intense ultraviolet radiation are phenomena associated with YSOs. General reviews of shocks have been given by Draine & McKee (1993) and Hollenbach (1997), and of PDRs by Hollenbach & Tielens (1997, 1998) and Sternberg (1998). ISO provides a variety of diagnostics of these regions. The pure rotational lines of H_2 form one of the most important tools, since they constrain directly the column density and temperature of the warm gas. In contrast, the vibration-rotation lines of H_2 at 2 μm probe only a small fraction of the warm gas ($\sim$ 1% or less), and require detailed models to infer the physical parameters. Other useful diagnostics include the CO and H_2O lines discussed above, as well as atomic and ionic fine-structure lines.

The pure rotational lines of H_2 are readily observed with the ISO-SWS up to high-J levels in PDRs and shocks (see, for example, Figures 2 and 10). In addition, the vibration-rotation lines at 2.4–4 μm are often detected. The analysis of these data usually proceeds through an excitation diagram, in which the logarithm of the column density divided by the statistical weight is plotted against the excitation energy of the level. For both PDRs and shocks, the pure rotational lines are generally fitted by two temperature components (see Timmermann et al. 1996, Wright et al. 1996, van den Ancker et al. 1998 for examples). The lower rotational lines with $J_u = 3 - 7$ indicate typically $T_{\rm rot} \sim$ 500 K for PDRs and $\sim$ 700 K for shocks. The higher rotational lines in shocks reflect temperatures of $\sim$ 2000 – 3000 K. In both PDRs and shocks, the excitation temperature characterizing the vibrational populations is $\sim$ 2000 K, but for PDRs the rotational excitation in $v > 0$ is given by a lower temperature, similar to that in v=0. Thus, PDRs and shocks can be distinguished by their H_2 emission, although the differences are subtle if only the pure rotational lines in v=0 are observed. An overview of the rotational temperatures derived from PDR and shock models is presented in Fig. 13 (van den Ancker et al. 1998).

The ISO observations of H_2 in a few well-characterized PDRs have been discussed by Timmermann et al. (1996), Bertoldi (1997) and Thi et al. (1999a), and are reviewed by Draine & Bertoldi (these proceedings). Published results have been limited mostly to PDRs with strong H_2 lines ($\sim$ 10 – 20 Jy), corresponding to regions with densities $n_{\rm H} > 10^4$ cm^{-3} and radiation fields $G_o > 100$ such as reflection nebulae. Maps of the higher-J lines at arcsec resolution have been made with ISOCAM (e.g., Boulanger et al. in preparation). The rotational temperature reflects directly the kinetic temperature structure of the gas, since the lower rotational lines are populated primarily by collisions. Observations of the S(0) line are important to constrain the lower end of the temperature gradient. The high vibrational temperature is due to ultraviolet pumping of the excited states (see e.g., Black & van Dishoeck 1987, Sternberg & Dalgarno 1989). Existing PDR models generally compute temperatures which are lower at the edge of the cloud than inferred from the ISO H_2 data. Possible solutions to this problem are mentioned by Bertoldi (1997) and Draine (these pro-

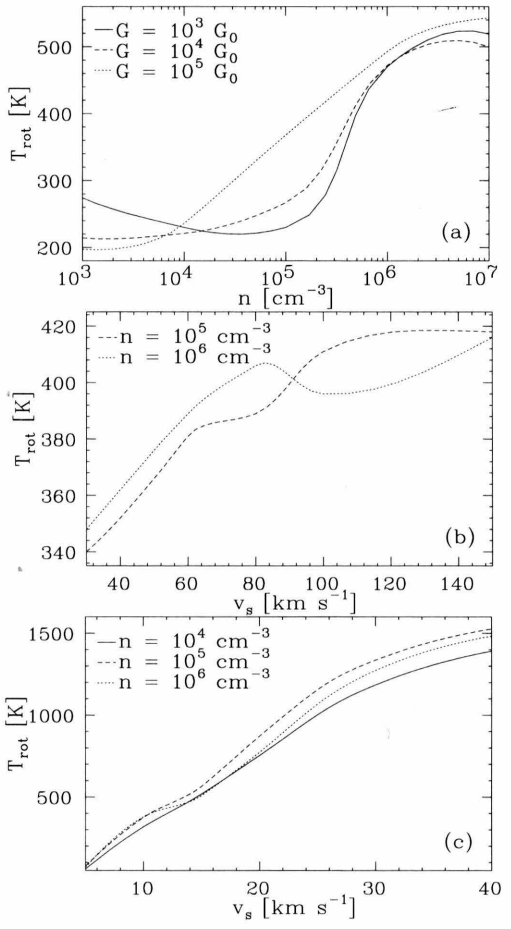

Figure 13. H_2 rotational temperatures derived from a) PDR models, b) J-shock models, and c) C-shock models. Note the relatively narrow range of T_{rot} expected for PDRs and J-shocks, but the broad range for C-shocks (van den Ancker et al. 1998).

ceedings). The ortho/para ratio is usually in LTE, as discussed by Sternberg & Neufeld (1999).

The best studied shock in the Galaxy is that associated with the Orion high-velocity outflow. The H_2 data centered at IRc2 are presented by van Dishoeck et al. (1998a) and Wright et al. (1999a), and those centered at peak I by Rosenthal et al. (these proceedings). Other examples discussed in the literature include the Cep A shock (Wright et al. 1996, van den Ancker et al. 1998), the DR 21 shock (Wright et al. 1997a) and HH 54 (Neufeld et al. 1998). In all cases, the data require two components with excitation temperatures of ~700 K and ~2000 K, respectively. Comparison with the models by Kaufman & Neufeld (1996) indicates that a mixture of slow- and fast C-shocks, and in some cases a J-shock as well, is necessary to explain the data. Such a mixture of shocks could reflect the fast direct impact and the slower oblique shocks expected for outflows. Further studies of weaker shocks are necessary to test whether this is a general phenomena, or whether it reflects limitations in the current models. The ortho/para ratio in shocks is generally equal to the high-temperature value of 3:1, except in the case of HH 54, where the lower value reflects an earlier colder phase of the gas.

ISOCAM–CVF maps of the higher-J lines in outflows at arcsec resolution have been presented by Cabrit et al. (these proceedings). The H_2 data form an interesting complement to CO interferometric data and provide constraints on the entrainment mechanism.

Near YSOs, a mixture of PDRs and shocks will generally occur. An interesting case where both may contribute equally is formed by the Herbig Ae/Be stars. Wesselius et al. (1996) and van den Ancker et al. (1998) have observed a large sample of these objects, and use diagnostics such as shown in Fig. 13 to distinguish the dominant excitation mechanism. In these mixed cases, the atomic and ionic lines provide good additional diagnostics. Specifically, the [Si II] 34.8 μm and [Fe II] 26.0 μm lines are strong in PDRs, whereas the [S I] 25.2 μm line becomes detectable only in shocks.

The [C II] 158 μm/ [O I] 63 μm and [O I] 63 μm/145 μm line ratios can also be used to distinguish PDRs and shocks, as well as low-velocity C- and high-velocity J-type shocks. The [O I] 63 μm emission in embedded, low-luminosity YSOs appears primarily due to shocks associated with the outflows, whereas the atomic lines in higher-mass Herbig Ae/Be objects have additional contributions from the PDRs (Saraceno et al., these proceedings).

7. CIRCUMSTELLAR DISKS AROUND YOUNG STARS

One of the most significant advances in recent years in the study of star-formation has been the detection and imaging of the dust continuum and CO line emission in circumstellar disks around young stars with millimeter interferometers (e.g., Koerner & Sargent 1995, Dutrey et al. 1996, Hogerheijde et al. 1997, Mannings & Sargent 1997). The typical sizes of the disks are ~100–400 AU, comparable to that of our own solar system. In order to study the evolution of the dust and gas in such disks, spectroscopy at infrared wavelengths is essential.

7.1. Solid-state features

ISO-SWS and LWS spectroscopy of circumstellar disks has been limited to the intermediate mass Herbig Ae stars because of the sensitivity of the instruments. An overview of the results is presented by Waelkens et al. (these proceedings). The disks around lower-mass T Tauri stars have only been studied with ISOPHOT-S spectroscopy (see Robberto et al., these proceedings). Nevertheless, the data on intermediate mass stars have provided a first glimpse of the richness and variety of solid-state spectral features in these objects. A beautiful example is presented by the case of HD 100546, where PAHs and crystalline silicates, in particular forsterite (Mg_2SiO_4), are detected (Waelkens et al. 1996, Malfait et al. 1998). The spectrum of the dust in this disk greatly resembles that of comet Hale-Bopp (Crovisier et al. 1997). The connection between interstellar and cometary material is also strengthened by the similarity in the composition of the ices (e.g., Bockelée-Morvan 1997, Ehrenfreund 1999).

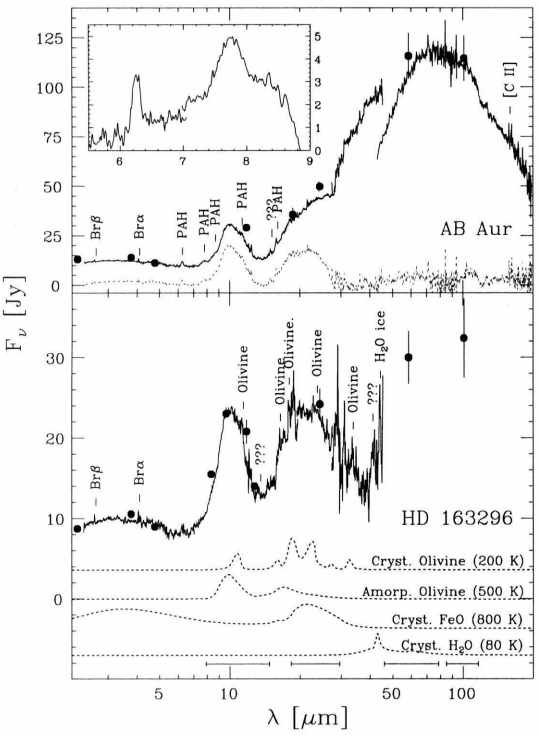

Figure 14. ISO spectra of AB Aur and HD 163296. The solid dots indicate ground-based and IRAS photometry, and the bars at the bottom of the figure indicate the IRAS passbands. The dashed line is the AB Aur spectrum after subtracting a smooth continuum, and the inset shows the UIR/PAH bands. The dashed lines at the bottom are the emissivities of various dust components at a given temperature. Note the prominent FeO emission in the HD 163296 spectrum and the continuum-subtracted AB Aur spectrum (van den Ancker et al. 1999).

Examples of spectra of other disks are shown in Fig. 14 for AB Aur and HD 163296 (van den Ancker et al. 1999). These stars have similar stellar characteristics and ages, but show very different mid-infrared features. The dust around AB Aur is dominated by warm amorphous olivines and crystalline iron oxides, with PAH features detected. In contrast, the disk around HD 163296 shows no PAHs but has a small fraction of crystalline olivines in addition to crystalline FeO, and the bulk of the amorphous silicates is colder than in AB Aur. In addition, H_2O ice is detected in this object. Thus, the dust spectral characteristics show no obvious trend with age, but may reflect local processes caused, for example, by the presence of nearby companions or the possible formation of planetary bodies. The case of HD 163296 also shows that spectroscopy is essential and that conclusions based on the fitting of the spectral energy distribution from broad-band photometry may lead to erroneous conclusions.

7.2. Gaseous species

An important question in the evolution of disks and the formation of giant planets is the time-scale over which the gas disappears from the disk. Previous studies have been based on millimeter observations of CO (e.g., Zuckerman et al. 1995, Dutrey et al. 1996), but the analysis of these data suffers from optical depth effects in the lines and possible freeze-out of the molecule onto grains in the coldest regions. The lowest H_2 pure rotational lines provide a powerful complement to the CO observations, since they directly measure the amount and temperature of the gas, although they can only be detected from warmer regions with $T \geq 60$ K.

Deep searches for the H_2 S(0) and S(1) lines have been performed with the ISO-SWS toward a dozen young stars with confirmed circumstellar disks (van Dishoeck et al. 1998c, Thi et al. 1999b). These objects were chosen to be isolated objects removed from molecular clouds, so that contamination from surrounding cloud emission is minimal. The S(1) line has been detected in most sources at the level of 0.3–1 Jy, whereas the S(0) line is seen in at least 2 objects. Analysis of the data suggests that a few % of the gas mass is at a temperature of ~100 K, which is higher than that suggested by disk models based on the CO emission alone. A survey by Stapelfeldt et al. (these proceedings) detected H_2 lines in 2 out of 12 sources, whereas data by Becklin et al. (this conference, see Thi et al. 1999b) show a possible S(1) line in 1 out of 2 sources. LWS spectra of some of the same objects by Creech-Eakman et al. (1999) reveal weak [C II] 158 μm emission, but no other atomic or molecular lines. The fraction of [C II] emission associated with the disks rather than the general diffuse interstellar medium remains to be determined.

8. CONCLUSIONS AND FUTURE PROSPECTS

ISO has provided important new tools for studying the physical and chemical structure of the envelopes around young stellar objects. These regions are well suited for ISO spectroscopy, because the high temperatures and densities result in bright infrared lines of atoms, ions and molecules such as H_2, H_2O and CO. In addition, absorption spectroscopy against embedded sources allows the colder gas and dust, in particular the ices, to be studied. Together, the spectral features allow a detailed picture of the evolution of the gas and dust around YSOs to be developed. The ISO observations of circumstellar disks provide strong support for a close connection between the interstellar and solar system material.

The ISO-SWS and LWS have given the first complete overview of the rich spectroscopy infrared wavelengths. The interpretation of the ISO data for YSOs is hindered, however, by insufficient spatial and spectral resolution, as well as sensitivity. What are the prospects to continue and improve on these studies in the future? Mid-infrared spectrometers on ground-based 8–10 m telescopes such as VISIR on the VLT will have comparable sensitivity to the SWS in atmospheric windows, but much better spatial and spectral resolution. Together with instruments on SOFIA they will be well suited to pursue observations of selected lines in YSOs and disks. The IRS on SIRTF, operating at 10–38 μm, will have up to a factor of 1000 better sensitivity than the ISO-SWS, but suffers from low spectral resolution ($\lambda/\Delta\lambda = 600$). Nevertheless, it will be a very powerful instrument to probe the solid-state features over a wide wavelength

range in a variety of objects. The heterodyne instruments on SOFIA and FIRST will provide important spectrally resolved information on H_2O, high-J CO, and other molecular lines at far-infrared and submillimeter wavelengths in YSOs. The largest gain in both sensitivity and spatial resolution at mid-infrared wavelengths will potentially be provided by a spectrometer on board NGST. ISO has paved the way for the exciting science to be performed with these new instruments in the coming decade.

REFERENCES

Baluteau, J.P., Cox, P., Cernicharo, J., et al. 1997, A&A, 322, L33

Bertoldi, F. 1997, in First ISO Workshop on Analytical Spectroscopy, ESA SP-419, p. 67

Black, J.H., van Dishoeck, E.F. 1987, ApJ, 322, 412

Bockelée–Morvan, D. 1997, in Molecules in Astrophysics: Probes and Processes, IAU Symposium 178, ed. E.F. van Dishoeck (Dordrecht: Kluwer), p. 219

Boogert, A.C.A., Helmich, F.P., van Dishoeck, E.F., Schutte, W.A., Tielens, A.G.G.M., Whittet, D.C.B. 1998, A&A, 336, 352

Boogert, A.C.A., Ehrenfreund, P., Gerakines, P., et al. 1999, A&A, in press

Boonman, A.M.S., Wright, C.M., van Dishoeck, E.F. 1999, to be submitted

Carr, J., Evans, N.J., Lacy, J.H., Zhou, S. 1995, ApJ, 450, 667

Ceccarelli, C., Caux, E., White, G.J., et al. 1998, A&A, 331, 372

Cernicharo, J., González-Alfonso, E., Alcolea, J., Bachiller, R., John, D. 1994, ApJ, 432, L59

Cernicharo, J., González-Alfonso, E., Lefloch, B. 1997a, in First ISO Workshop on Analytical Spectroscopy, ESA SP-419, p. 23

Cernicharo, J., Lim, T., Cox, P. et al. 1997b, A&A, 323, L25

Charnley, S.B. 1997, ApJ, 481, 396

Creech-Eakman, M., Blake, G.A., van Dishoeck, E.F., et al. 1999, in preparation

Crovisier, J., Leech, K., Bockelée-Morvan, D., et al. 1997, Science, 275, 1904

Dartois, E., d'Hendecourt, L., Boulanger, F., Jourdain de Muizon, M., Breitfellner, M., Puget, J-L, Habing, H.J. 1998, A&A, 331, 651

Dartois, E., Schutte, W.A., Geballe, T., et al. 1999, A&A, in press

de Graauw, Th., Whittet, D.C.B., Gerakines, P.A., et al. 1996, A&A, 315, L345

Demyk, K., Dartois, E., d'Hendecourt, L., Jourdain de Muizon, M., Heras, A.M., Breitfellner, M. 1998, A&A, 339, 553

d'Hendecourt, L.B., Jourdain de Muizon, M., Dartois, E. et al. 1996, A&A, 315, L365

Doty, S.D., Neufeld, D.A. 1997, ApJ, 489, 122

Draine, B.T., McKee, C.F. 1993, ARAA, 31, 373

Dutrey, A., Guilloteau, S., Duvert, G., et al. 1996, A&A, 309, 493

Ehrenfreund, P. 1999, in Cometary Nuclei in Space and Time, IAU Colloquium 168, ed. M. A'Hearn, in press

Ehrenfreund, P., Boogert, A.C.A., Gerakines, P.A., et al. 1997, in First ISO Workshop on Analytical Spectroscopy, ESA SP-419, p. 3

Ehrenfreund, P., Boogert, A., Gerakines, P., Tielens, A.G.G.M. 1998a, Far. Disc., 109, 463

Ehrenfreund, P., Dartois E., Demyk K., d'Hendecourt L. 1998b, A&A 339 L17

Evans, N.J., Lacy, J.H., Carr, J.S. 1991, ApJ, 383, 674

Genzel, R., Lutz, D., Sturm, E., et al. 1998, ApJ, 498, 579

Gerakines, P.A., Whittet, D.C.B., Ehrenfreund, P., et al. 1999, ApJ, in press

Gibb, E., Whittet, D.C.B. et al. 1999, in preparation

González-Alfonso, E., Cernicharo, J., van Dishoeck, E.F., Wright, C.M., Heras, A. 1998, ApJ, 502, L169

Guertler, J., Henning, Th., Kömpe, C., et al. 1996, A&A, 315, L189

Harwit, M., Neufeld, D.A., Melnick, G.J., Kaufman, M.J. 1998, ApJ, 497, L105

Helmich, F.P., van Dishoeck, E.F., Black, J.H. et al. 1996, A&A, 315, L173

Heras, A.M., Leech, K., Trams, N.R., Perry, M., eds. 1997, First ISO Workshop on Analytical Spectroscopy, ESA-SP 419 (Noordwijk: ESTEC)

Hogerheijde, M.R. 1998, PhD thesis, University of Leiden

Hogerheijde, M.R., van Langevelde, H.J., Mundy, L.G., Blake, G.A., van Dishoeck, E.F. 1997, ApJ, 490, L99

Hollenbach, D.J. 1997, in Herbig-Haro Objects and the Birth of Low-mass Stars, IAU Symposium 182, ed. B. Reipurth and C. Bertout (Dordrecht: Kluwer), p. 181

Hollenbach, D.J., Tielens, A.G.G.M. 1997, ARAA 35, 179

Hollenbach, D.J., Tielens, A.G.G.M. 1998, Rev. Mod. Phys., in press

Kaufman, M.J., Neufeld, D.A. 1996, ApJ, 456, 611

Kaufman, M.J., Hollenbach, D.J. and Tielens, A.G.G.M. 1998, ApJ, 497, 276

Koerner, D.W., Sargent, A.I. 1995, AJ, 109, 2138

Lahuis, F., van Dishoeck, E.F., 1997, in First ISO Workshop on Analytical Spectroscopy, ESA SP-419, p. 275

Lahuis, F., van Dishoeck, E.F., 1999, A&A, in preparation

Langer, W.D., van Dishoeck, E.F., Blake, G.A. et al. 1999, in Protostars & Planets IV, eds. V. Mannings, A.P. Boss and S.S. Russell, (Tucson: Univ. Arizona), in press

Liseau, R., Ceccarelli, C., Larsson, B. et al. 1996, A&A, 315, L181

Malfait, K., Waelkens, C., Waters, L.B.F.M., et al. 1998, A&A, 332, L25

Mannings, V., Sargent, A.I. 1997, ApJ, 490, 792

Melnick, G.J., Stauffer, J.R., Ashby, M., et al. 1999, AAS meeting 193, 72.01; and in preparation.

Meyer, D.M., Jura, M., Cardelli, J.A. 1998, ApJ, 493, 222

Mitchell, G.F., Maillard, J.–P., Allen, M., Beer, R., Belcourt, K. 1990, ApJ, 363, 554

Neufeld, D.A., Kaufman, M.J 1993, ApJ, 418, 263

Neufeld, D.A., Melnick, G.J., Harwit, M. 1998, ApJ, 506, L75

Nisini, B., Giannini, T., Molinari, S., et al. 1998, in Star Formation with ISO, eds. J. Yun & R. Liseau, ASP vol. 132, p. 256

Nisini, B., Benedettini, M., Giannini, T., et al. 1999a, A&A, in press

Nisini, B., Benedettini, M., Giannini, T., et al. 1999b, A&A, submitted

Olofsson, G., Pagani, L., Tauber, J., et al. 1998, A&A, 339, L81

Roelfsema, P., Cox, P., Tielens, A.G.G.M., et al. 1996, A&A, 315, L289

Saraceno, P., Benedettini, M., Di Giorgio, A.M., et al. 1999, in Physics and Chemistry of the Interstellar Medium III, eds. V. Ossenkopf et al. (Berlin: Springer), in press

Schutte, W.A. 1999, in Laboratory Astrophysics and Space Research, ed. P. Ehrenfreund et al. (Dordrecht: Kluwer), p. 69

Schutte, W.A., Boogert, A.C.A., Tielens, A.G.G.M., et al. 1999, A&A, in press

Schutte, W.A., Tielens, A.G.G.M., Whittet, D.C.B., et al. 1996, A&A, 315, L333

Shu, F.H., Najita, J., Galli, D., Ostriker, E., Lizano, S. 1993, in Protostars & Planets III, ed. E.H. Levy, J. Lunine (Tucson: Univ. Arizona), p. 3

Sternberg, A. 1998, in The Molecular Astrophysics of Stars and Galaxies, eds. T.W. Hartquist and D.A. Williams (Oxford: OUP), p. 201

Sternberg, A., Dalgarno, A. 1989, ApJ, 338, 197

Sternberg, A., Neufeld, D.A. 1999, ApJ, in press

Strazzulla, G., Nisini, B., Leto, G., Palumbo, M.E., Saraceno, P. 1998, A&A, 334, 1056

Thi, W.F., van Dishoeck, E.F., Jansen, D.J., Spaans, M., Li, W., Evans, N.J., Jaffe, D.T. 1997, in First ISO Workshop on Analytical Spectroscopy, ESA SP-419, p. 299

Thi, W.F., van Dishoeck, E.F., Black, J.H., et al. 1999a, these proceedings

Thi, W.F., van Dishoeck, E.F., Blake, G.A. et al. 1999b, these proceedings

Tielens, A.G.G.M., Hagen, W. 1982, A&A, 114, 245

Tielens, A.G.G.M., Whittet, D.C.B. 1997, in Molecules in Astrophysics: Probes and Processes, IAU Symposium 178, ed. E.F. van Dishoeck (Dordrecht: Kluwer), p. 48

Tielens, A.G.G.M., Tokunaga, A.T., Geballe, T.R., Baas, F. 1991, ApJ, 381, 181

Timmermann, R., Bertoldi, F., Wright, C.M., Drapatz, S., Draine, B.T., Haser, L., Sternberg, A. 1996, A&A, 315, L281

van den Ancker, M.E., Wesselius, P.R., Tielens, A.G.G.M., Waters, L.B.F.M. 1998, in ISO's view on stellar evolution, Astrophys. Spa. Sci., 255, p. 69

van den Ancker, M.E., Bouwman, J., Wesselius, P.R., Waters, L.B.F.M., Dougherty, S.M., van Dishoeck, E.F. 1999, A&A, in press

Vandenbussche, B., Ehrenfreund, P., Boogert, A.C.A. et al. 1999, A&A, submitted

van der Tak, F.F.T., van Dishoeck, E.F., Evans, N.J., Blake, G.A. 1999, ApJ, in press

van Dishoeck, E.F. 1998, Far. Disc., 109, 31

van Dishoeck, E.F., Blake, G.A. 1998, ARAA, 36, 317

van Dishoeck, E.F., Helmich, F.P. 1996, A&A, 315, L177

van Dishoeck, E.F., Hogerheijde, M.R. 1999, in The Physics of Star Formation and Early Stellar Evolution, eds. C.J. Lada and N. Kylafis (Dordrecht: Kluwer), in press

van Dishoeck, E.F., Helmich, F.P., de Graauw, Th. et al. 1996, A&A, 315, L349

van Dishoeck, E.F., Wright, C.M., Cernicharo, J., González-Alfonso, E., Helmich, F.P., de Graauw, Th., Vandenbussche, B. 1998a, ApJ, 502, L173

van Dishoeck, E.F., Helmich, F.P., Schutte, W.A., et al. 1998b, in Star Formation with ISO, eds. J. Yun & R. Liseau, ASP vol. 132, p. 54

van Dishoeck, E.F., Thi, W.F., Blake, G.A., Mannings, V., Sargent, A.I., Koerner, D., Mundy, L.G. 1998c, in ISO's View on Stellar Evolution, Astrophys. Spa. Sci., 255, 77

Waelkens, C., Waters, L.B.F.M., de Graauw, Th., et al. 1996, A&A, 315, L245

Waters, L.B.F.M., Waelkens, C., van der Hucht, K.A., Zaal, P.A., eds. 1998, ISO's view on Stellar Evolution (Dordrecht: Kluwer), Astrophys. Spa. Sc. vol. 255

Wesselius, P.R., van den Ancker, M.E., Young, E.T., et al. 1996, A&A, 315, L197

Whittet, D.C.B., Schutte, W.A., Tielens, A.G.G.M. et al. 1996, A&A, 315, L357

Willner, S.P., Gillett, F.C., Herter, T.L. et al. 1982, ApJ, 253, 174

Wright, C.M., Drapatz, S., Timmermann, R., van der Werf, P.P., Katterloher, R., de Graauw, Th. 1996, A&A, 315, L301

Wright, C.M., Timmermann, R., Drapatz, S. 1997a, in First ISO Workshop on Analytical Spectroscopy, ESA SP-419, p. 311

Wright, C.M., van Dishoeck, E.F., Helmich, F.P., Lahuis, F., Boogert, A.C.A., de Graauw, Th. 1997b, in First ISO Workshop on Analytical Spectroscopy, ESA SP-419, p. 37

Wright, C.M., van Dishoeck, E.F., et al. 1999a, A&A, to be submitted

Wright, C.M., van Dishoeck, E.F., Feuchtgruber, H., Cernicharo, J., González-Alfonso, E., Black, J.H., de Graauw, Th. 1999b, ApJ, to be submitted

Yun, J., Liseau, R. 1998, Star Formation with the Infrared Space Observatory, ASP vol. 132 (San Francisco: ASP)

Zmuidzinas, J., Blake, G.A., Carlstrom, J., et al. 1995. In Proceedings of the Airborne Astronomy Symposium, ed. M.R. Haas, J.A. Davidson, E.F. Erickson, (San Francisco: ASP), p. 33

Zuckerman, B., Forveille, T., Kastner, J.H. 1995, Nature, 373, 494